Charge Distribution and Optical Transitions of Tetraalkyl Diazenium Dications

Stephen F. Nelsen* and Yichun Wang

Contribution from the S. M. McElvain Laboratories of Organic Chemistry,
Department of Chemistry, University of Wisconsin, 1101 West University Avenue,
Madison, Wisconsin 53706-1396

Received June 13, 1994®

Abstract: Calculations at the MP2/6-31G* level for 2,7-diazatetracyclo[6.2.2.2^{3,6}]tetradecane dication ($\mathbf{1}^{2+}$) give charges at each nitrogen of +0.06, at each $C_\alpha H$ group of +0.23, and at each $C_\beta H_2$ group of +0.12. The increases in charge upon removal of two electrons from the neutral hydrazine are +0.86 at both nitrogens, +0.23 at all four $C_\alpha H$ groups, and +0.91 at all eight $C_\beta H_2$ groups. The near-UV optical spectra of $\mathbf{1}^{2+}$ and $\mathbf{3}^{2+}$ show broad long-wavelength absorption near 300 nm ($\epsilon \sim 1700\ M^{-1}\ cm^{-1}$ between ~295 and 320 nm for $\mathbf{1}^{2+}$ and $\mathbf{3}^{2+}$) and stronger short-wavelength absorption (ϵ 5500 at 230 nm for $\mathbf{1}^{2+}$ and $\epsilon \sim 3100$ at 222 nm for $\mathbf{3}^{2+}$). Clark and Chandrasekar's configuration interaction method using AM1 calculations predicts that the long-wavelength band should be assigned to a $\sigma \rightarrow \pi^*$ transition and that more intense $\sigma \rightarrow \pi^*$, $\pi \rightarrow \pi^*$, and $\sigma \rightarrow \sigma^*$ transitions all might contribute to the shorter-wavelength band. Comparisons of CIS/6-31G* and CC-CI/AM1 calculations on tetramethylhydrazine dication show good agreement of orbital ordering and oscillator strengths, but very poor agreement of transition energies ($\pi \rightarrow \pi^*$ calculated at 151 and 265 nm, respectively).

Introduction

Removal of two electrons from a tetraalkylhydrazine produces the diazenium dication **A**, which has a π bond centered at two formally positively charged nitrogen atoms. The unusual $^+N{=}N^+$ functional group makes diazenium dications very reactive, and most examples of **A** have extremely short lifetimes in solution because of rapid loss of an α-proton to produce imino-alkylated hydrazone cations **B**. Incorporation of the alkyl groups into bis(*N,N'*-bicycloalkyl) rings, the "sesquibicyclic" substitution pattern, greatly increases dication lifetime by a Bredt's rule effect: the polycyclic structure forces twisting of the $C{=}N^+$ bond of **B**, which destabilizes it and effectively slows deprotonation of **A**. Many sesquibicyclic examples of **A** have lifetimes of seconds in acetonitrile,[1] but their reactivity is strongly dependent upon bicyclic ring size. For convenience we will designated bicyclic ring size using the number of carbons in the two bridges present in addition to the two-nitrogen bridge which is common to all. The least reactive example of **A** is the <u>22/22</u> dication $\mathbf{1}^{2+}$, which is stable for days at room temperature in acetonitrile and isolable as its $(BF_4^-)_2$ and $(PF_6^-)_2$ salts.[1,2] $\mathbf{1}^{2+}$ exhibits near-UV absorption bands, at least one of which presumably represents hydrocarbon framework, $^+N{=}N^+$ transitions. Although C_α deprotonation is effectively inhibited for $\mathbf{1}^{2+}$ by the Bredt's rule effect, it is an unusually strong C–H acid, and it is deprotonated at C_β to produce the amino-aziridinium cation **2** by bases as weak as chloride in acetonitrile.[3] Both enlarging and contracting one of the <u>22</u> bridges of $\mathbf{1}^{2+}$ leads to increased reactivity. C_α acidity increases markedly when a bridge is enlarged. The <u>22/23</u> dication $\mathbf{3}^{2+}$ is α-deprotonated slowly by water in acetonitrile, and the <u>22/24</u> dication $\mathbf{4}^{2+}$ is quenched by diethyl ether at −33 °C to give an isolable example of **B**.[4] Incorporation of a <u>21</u> ring in $\mathbf{5}^{2+}$ results in an increase in C_β–H acidity relative to $\mathbf{1}^{2+}$, and only the *exo* <u>21</u> hydrogens (shown on the structure as H_x) are removed by pyridine. Even in the absence of base, $\mathbf{5}^{2+}$ is unstable because it alkylates acetonitrile, undergoing C_α–N cleavage in an S_N2 reaction having a half-life of about 5 min at room temperature.[5] This reaction has a lower barrier than does methylation of acetonitrile by $MeOSO_2F$, implying that $^+N{=}N^+$ is an exceptionally powerful leaving group. The more highly strained <u>21/</u>

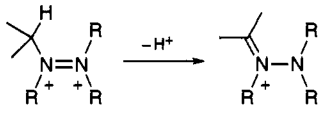

A **B**

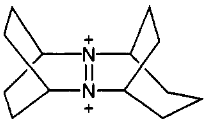

$\mathbf{3}^{2+}$

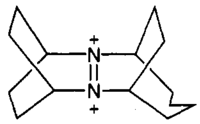

$\mathbf{4}^{2+}$

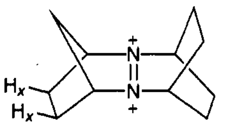

$\mathbf{5}^{2+}$

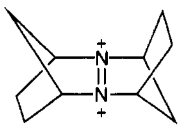

$\mathbf{6}^{2+}$

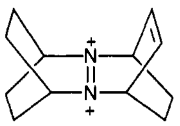

$\mathbf{7}^{2+}$

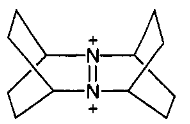

$\mathbf{1}^{2+}$

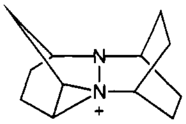

2

® Abstract published in *Advance ACS Abstracts,* April 15, 1995.

[1] (a) Nelsen, S. F.; Blackstock, S. C.; Frigo, T. B. *J. Am. Chem. Soc.* **1984,** *106,* 3366. (b) Nelsen, S. F.; Blackstock, S. C.; Frigo, T. B. *Tetrahedron* **1986,** *42,* 1769. (c) Nelsen, S. F.; Frigo, T. B.; Kim, Y. *J. Am. Chem. Soc.* **1989,** *111,* 5387.

[2] Nelsen, S. F.; Blackstock, S. C.; Haller, K. J. *Tetrahedron* **1986,** *42,* 6101.

[3] Nelsen, S. F.; Wang, Y. *J. Am. Chem. Soc.* **1991,** *113,* 5905.

[4] Nelsen, S. F.; Wang, Y. *J. Am. Chem. Soc.* **1992,** *114,* 7923.

0002-7863/95/1517-5341$09.00/0

21 compound **6**$^{2+}$ is far more reactive toward C$_\alpha$−N cleavage, and has a sub-millisecond lifetime at room temperature in acetonitrile. Significant ring strain is not necessary for rapid C$_\alpha$−N cleavage; the allylic bond weakening accompanying incorporation of an unsaturated u22 bridge in **7**$^{2+}$ results in a half-life for C$_\alpha$−N$^+$ cleavage in acetonitrile of about 1 min at room temperature.[5]

This paper discusses the results of calculations carried out in attempts to better understand the unusual reactivities and optical spectra caused by the $^+$N═N$^+$ functional group as the substituents are changed.

Experimental and Calculated Geometries for Sesquibicyclic Hydrazine Dications

The N═N bond length does not change very much upon alkylation of the nitrogen lone pairs of the 22 bicyclic azo compound **8**, for which d(N═N) = 1.255(4) Å.[6] The dimeric mono-N-alkylated analogue **9**$^{2+}$(BF$_4^-$)$_2$ has eight crystallographically different $^+$N═N units which vary in d(N═N) from 1.241(4) to 1.261(4) Å, the larger values being associated with closest fluorine to disubstituted nitrogen approach slightly under the van der Waals sum of N and F distances of 3.02 Å, and NNF angle near 95°.[7] **1**$^{2+}$(**PF**$_6^-$)$_2$ has d(N═N) = 1.270(5) Å,[2] only slightly larger than those of **8** and **9**$^{2+}$. An X-ray structure of the only other isolated hydrazine dication salt, **3**$^{2+}$(**PF**$_6^-$)$_2$ · 2(CH$_3$CN), has d(N═N) = 1.247(10) Å, 0.023 Å shorter than that of **1**$^{2+}$, but the crystal is severely disordered.[8] The **3**$^{2+}$ dication unit is at a center of symmetry in the crystal, requiring that the 23 bridges are equally oriented in two directions, making only structural parameters averaged over the 22 and 23 bridges available and precluding accurate comparison with calculated structures.

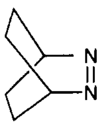

8

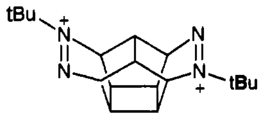

9^{2+}

The nitrogens of diazenium dications are planar both crystallographically and by all methods of calculation. Crystalline **1**$^{2+}$(**PF**$_6^-$)$_2$ has only one type of N and C$_\alpha$, but two types of C$_\beta$, while all calculations optimize isolated **1**$^{2+}$ to D_{2h} symmetry, with only one type of C$_\beta$. Table 1 compares the geometries obtained by *ab initio* calculations at the RHF/6-31G* (abbreviated RHF) and MP2/6-31G* (abbreviated MP2) levels and by AM1 semiempirical calculations with that obtained by X-ray. The RHF structure of **1**$^{2+}$ is disappointingly poor, with the N═N bond length underestimated by 0.053 Å (4.2%) and the C−N bond length overestimated by 0.037 Å (2.5%). The problem that *ab initio* calculations have with predicting the dication geometry appears to be principally an overcorrection of the effects of electron correlation at the MP2 level because MP2 geometry optimization makes substantial changes in geometry, d(NN) increasing by 0.093 Å and d(NC) decreasing by 0.054 Å. Unfortunately, these changes are too large, and MP2 gives d(NN) 0.04 Å too long and d(NC) 0.02 Å too short. MP2 geometry optimization of neutral **1** gives the X-ray geometry at nitrogen,[9] suggesting to us that electron correlation effects are more important in the dication. AM1 calculations on **1**$^{2+}$ give a geometry as close to that of the X-ray structure as the MP2/6-31G* *ab initio* calculation, in great contrast to neutral **1**, for which AM1 severely underestimates d(NN). AM1 calculations clearly do a rather poor job on lone pair electrons, and removing them in oxidized forms significantly improves the geometries obtained. The principal error the AM1 calculation makes in the geometry of **1**$^{2+}$ is to give d(CN) 0.04 Å too long: all the other geometrical parameters are quite close to the experimental values. The far more rapid semiempirical AM1 calculations do a better job at predicting the geometry of **1**$^{2+}$ than do *ab initio* calculations at the RHF level, and as good a job as do MP2 calculations.

Table 1. Comparison of Geometries Calculated for **1**$^{2+}$ with the X-ray Structure

	X-ray	6-31G*	MP2/6-31G*	AM1
		Bond Lengths, Å		
d(NN)	1.270(5)	1.217(−0.053)	1.310(+0.040)	1.273(+0.003)
d(C$_\alpha$N)	1.471(3)	1.508(+0.037)	1.454(−0.017)	1.513(+0.042)
d(C$_\alpha$C)	1.543[a]	1.542(−0.001)	1.554(+0.011)	1.550(+0.007)
d(CC)	1.520[b]	1.544(+0.024)	1.533(+0.013)	1.523(+0.003)
		Bond Angles, deg		
∠(NNC$_\alpha$)	115.8(1)	116.2(+0.4)	115.4(−0.4)	115.2(−0.6)
∠(C$_\alpha$NC$_\alpha$)	128.5(2)	127.6(−0.9)	129.3(+0.8)	129.5(+1.0)
∠(C$_\alpha$CC)	109.5[c]	109.0(−0.5)	109.2(−0.3)	109.6(+0.1)
∠(NC$_\alpha$C)	105.9[d]	105.6(−0.3)	106.6(+0.7)	107.4(+1.5)
∠(CC$_\alpha$C)	110.2(2)	111.4(+1.2)	109.8(−0.4)	107.2(−3.0)

[a] Average of 1.547(3) and 1.539(3). [b] Average of 1.518(5) and 1.522(5). [c] Average of 109.4(1) and 109.6(1). [d] Average of 105.6(2) and 105.2(2).

MP2 calculations have also been carried out on **6**$^{2+}$ and RHF calculations on **10**$^{2+}$, both of which are far too unstable for isolation. The geometries at nitrogen thus obtained are compared with those for **1**$^{2+}$ and with other calculations in Table 2. It may be noted that *ab initio* calculations predict a decrease in d(N═N) for **6**$^{2+}$ relative to **1**$^{2+}$, while AM1 predicts an increase; it is not known experimentally which prediction is correct.

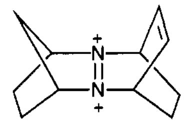

10^{2+}

Charges in Hydrazine Dications

The distribution of the charge introduced as electrons are removed is a point of particular interest for considering the chemistry of oxidized hydrazines. Both the bridgehead protons and carbons show substantial downfield shifts upon double electron removal from sesquibicyclic hydrazines: δ_H increases 3.1−3.5 ppm and δ_C 18−30 ppm for all cases studied.[5] The amount the signals for protons and carbons β to nitrogen move upon double electron removal varies widely. Comparing the spectrum of inverting neutral **1**, where the anisotropic effects on chemical shift are averaged, with that of **1**$^{2+}$, δ_H increases 0.46 ppm for both the exo and endo β-hydrogens, while δ_C increases 2.9 ppm. These shifts are 13.0 and 9.5% of the downfield shifts for the bridgehead (α) protons and carbons,

---

(5) Nelsen, S. F.; Wang, Y. *J. Org. Chem.* In press.

(6) Ottersen, T.; Romming, C.; Snyder, J. P. *Acta Chem. Scand. Ser. B* **1976**, *30*, 407.

(7) Nelsen, S. F.; Chang, H.; Wolff, J. J.; Powell, D. R. Submitted for publication.

(8) Because of disorder of both cations and anions in the structure of **3**$^{2+}$, BF$_4^-$ placement is uncertain, and even d(N═N) has rather large uncertainty. The closest N,F distance in **1**$^{2+}$(BF$_4^-$) is 3.50 Å, while for the most intense BF$_4^-$ in **3**$^{2+}$(BF$_4^-$) d(N,F) = 3.60 Å. It is still not clear how much BF$_4^-$ placement might be affecting d(N═N) in the diazenium dications; it causes a variation of about 0.02 Å for trialkyldiazenium monocations.[7]

(9) Nelsen, S. F.; Wang, Y.; Powell, D. R.; Hayashi, R. K. *J. Am. Chem. Soc.* **1993**, *115*, 5246.

Table 2. Comparison of Calculated Geometries at Nitrogen for $\mathbf{1}^{2+}$, $\mathbf{6}^{2+}$, and $\mathbf{10}^{2+}$

	$\mathbf{1}^{2+}$	$\mathbf{6}^{2+}$	$\mathbf{10}^{2+}$
d(NN), Å			
X-ray	1.270(5)		
AM1	1.273[+0.003]	1.281	1.278
RHF/6-31G*	1.217[−0.053]	1.211	1.212
MP2/6-31G*	1.310[+0.040]	1.304	
d(CN), Å			
X-ray	1.471(3)		
AM1	1.513[+0.042]	1.543	1.515 (u$\underline{22}$), 1.549 ($\underline{21}$)
RHF/6-31G*	1.508[+0.037]	1.523	1.525 (u$\underline{22}$), 1.507 ($\underline{21}$)
MP2/6-31G*	1.454[−0.017]	1.470	
∠(NNC), deg			
X-ray	115.8(1)		
AM1	115.2[−0.6]	109.05	115.3 (u$\underline{22}$), 108.9 ($\underline{21}$)
RHF/6-31G*	116.2[+0.4]	109.70	116.1 (u$\underline{22}$), 109.5 ($\underline{21}$)
MP2/6-31G*	115.4[−0.4]	108.78	
∠(CNC), deg			
X-ray	128.5(2)		
AM1	129.5[+1.0]	141.90	135.8
RHF/6-31G*	127.6[−0.9]	140.59	134.2
MP2/6-31G*	129.3[+0.8]	142.44	

Table 3. Calculated NPA Charges for **1** in the Neutral and Dication Oxidation States

	RHF/6-31G* SCF(NPA)	MP2/6-31G* SCF(NPA)	geometry: MP2(NPA)	semiempir. AM1(NPA)
neutral				
N	−0.415	−0.412	−0.371	−0.143
$C_\alpha H$	+0.204	+0.199[a]	+0.176	+0.060
$C_\beta H_2$	+0.002	+0.003[b]	+0.005	+0.006
dication				
N	+0.073	+0.057	+0.059	+0.093
$C_\alpha H$	+0.259	+0.247[c]	+0.233	+0.173
$C_\beta H_2$	+0.102	+0.113[d]	+0.119	+0.140
	Increase in Charge between Neutral and Dication			
both N	+0.98	+0.94	+0.86	+0.47
all $C_\alpha H$	+0.22	+0.20	+0.23	+0.45
all $C_\beta H_2$	+0.80	+0.86	+0.91	+1.07

[a] Charges: $C_\alpha(3)$ −0.02979, H +0.23376; $C_\alpha(5)$ −0.03772, H +0.23240. [b] Charges: C)3)$\underline{C}_\beta$(7,*outer*) −0.43341, H_x +0.21123, H_n +0.23423; C(3)$\underline{C}_\beta$(13,*inner*) −0.45750, H_x +0.22336, H_n +0.22057; C(5)$\underline{C}_\beta$9,*outer*) −0.43884, H_x +0.22007, H_n +0.24086; C(5)$\underline{C}_\beta$(11,*inner*) −0.45164, H_x +0.22590, H_n +0.21864. [c] Charges: C_α −0.05867, H +0.30534. [d] Charges: C_β −0.45381, H_x +0.29462, H_n +0.27169.

respectively. Neither proton nor carbon chemical shifts reflect only electron density, and the geometries change significantly upon oxidation because the nitrogens flatten, so it appears impossible to reliably infer the charge distribution from NMR data.

To estimate where the charge introduced upon oxidation appears, we have turned to calculations. Wiberg and Rablen have recently compared various methods of calculating atomic charges.[10] Table 3 shows the charges calculated for **1** in both neutral and dication oxidation states, averaged over the different types of C_α and C_β carbons present (the differences are rather small anyway). The carbon and attached hydrogen charges have been added to allow easier comparison of charge distribution. Mulliken charges from *ab initio* calculations are known to be incorrect for many systems[10,11] and are not shown in Table 3. Weinhold–Reed Natural Population Analysis (NPA) charges,[12] which employ orthogonal orbitals and avoid the numerical problems of Mulliken charges,[10,12] are significantly different from the Mulliken charges for the dication. As we have argued elsewhere,[13] the ring size effect on ease of first and second electron removal in solution makes it very likely that the charge at nitrogen of hydrazine dications is positive, as is the NPA charge; we shall only consider NPA charges here. Also included in Table 3 are the charges obtained from AM1 calculations. The AM1 calculations require on the order of 1/1000th of the computer time of RHF *ab initio* calculations, but they give poor NN bond lengths for neutral hydrazines and do not predict the bicyclic ring torsion which is experimentally observed for $\underline{22}$ systems.[9] Because semiempirical calculations ignore the core and use orthogonalized orbitals, they avoid the numerical problems of the Mulliken charge analysis, and AM1 gives NPA charges.[12c] It will be noted that the *ab initio* calculations give far more polarization of charge in the C_α–N bonds of the neutral form than do AM1 calculations, and the much better RHF geometries imply that the *ab initio* charges are likely to be more realistic. Differences between the two types of calculations are smaller for the dications. It may be noted that the $C_\beta H_2/C_\alpha H$ charge ratio for $\mathbf{1}^{2+}$ is estimated at 0.39, which is comparable to the 0.45 attenuation of charge estimated by Taft for insertion of a saturated carbon between a charged atom and a probe carbon.[14] The charge ratio of 0.81 obtained from the AM1 calculations is unreasonably high, and we conclude that AM1 calculations do not give very good charge distributions for these systems.[15] Calculations give very different charge distributions from the resonance structure formalism, which writes all of the positive charge at the nitrogens in the dication, and no charges in the neutral form. The total +2 charge of the dication is ≥93% delocalized onto the alkyl groups with the $C_\beta H_2$ groups assuming 44–51% of this charge, while the alkyl groups in the neutral form share a charge of +0.83 to +0.74, with the $C_\beta H_2$ groups assuming only 2–3% of this charge. Thus when two electrons are removed from neutral **1**, 0.98 to 0.86 come from the nitrogens, 0.20 to 0.23 from the $C_\alpha H$ groups, and 0.80 to 0.91 from the $C_\beta H_2$ groups. This type of charge distribution rationalizes the great acidity of the C_β–H bonds of $\mathbf{1}^{2+}$. Table 4 shows RHF *ab initio* NPA charges for the more complex $\underline{21}$/u$\underline{22}$ system $\mathbf{10}^{2+}$, where distribution between different ring sizes can be examined. Significantly more of the increase in charge in the hydrocarbon units, +0.31, appears at the $C_\alpha H$ positions

Table 4. Calculated NPA RHF/6-31G* Charges for **10** in the Neutral and Dication Oxidation States

	neutral	dication	increase[a]
N	−0.403	+0.071	+0.474
C_αH,u22	+0.177	+0.244	+0.067
$C_\beta H_v$u$\underline{22}$	−0.013	+0.096	+0.109
$C_\beta H_2$,u$\underline{22}$	+0.030	+0.122	+0.092
C_αH, 21	+0.201	+0.289	+0.088
$C_\beta H_2$,21	−0.016	+0.138	+0.154
$C_\beta H_2$,$\underline{2}$1	+0.016	+0.108	+0.092

[a] The increase in charge upon removing two electrons from the neutral compound, which sums to +0.95 at both N, +0.31 at all $C_\alpha H$, and +0.74 at all $C_\beta H_2$.

---

(10) Wiberg, K. B.; Rablen, P. R. *J. Comput. Chem.* **1993**, *14*, 1504.

(11) (a) Reed, A. E.; Weinstock, R. B.; Weinhold, F. *J. Chem. Phys.* **1985**, *83*, 735. (b) The 6-31G* geometry Mulliken charge at N for $\mathbf{1}^{2+}$ is −0.116, which we do not doubt is the wrong sign.

(12) (a) Reed, A. E.; Curtiss, L. A.; Weinhold, F. *Chem. Rev.* **1988**, *88*, 899. (b) Glendening, E. D.; Reed, A. E.; Carpenter, J. E.; Weinhold, F. *NBO 3.0 Program Manual Technical Notes*; WIS-TCI-756, Madison, 1990. (c) We thank Frank Weinhold for providing a program giving NPA analysis of AM1 calculations.

(13) We have not computed the AIM charges Wiberg prefers,[10] partially because these calculations are extremely time-consuming, but also because we believe the nitrogens would come out negatively charged using this method.

(14) Taft, R. W., Jr. *Steric Effects in Organic Chemistry*; Newman, M. S., Ed.; Wiley: New York, 1956; p 594.

(15) AM1 charges also look unreasonable for D_{2d} nBu_4N^+: sums over carbon and hydrogens give $CH_2(\alpha)$ +0.140, $CH_2(\beta)$ +0.028, $CH_2(\gamma)$ +0.025, $CH_3(\delta)$ +0.250. Even just comparing the methylene groups, the β charge is 20% of the α, while the γ is 91% of the β, which is not reasonable.

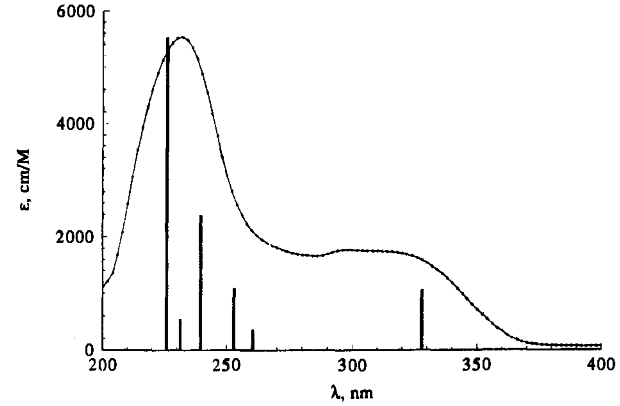

Figure 1. The experimental UV spectrum of $1^{2+}(PF_6^-)_2$ in acetonitrile is shown as dots connected by lines. The AM1-CC-CI-SCRF calculated transition energies for acetontrile (last line, Table 6) are shown as bars with the intensity of the strongest transition arbitrarily set to that of the observed spectrum (OS × 1.43 × 10^4).

of $\mathbf{10}^{2+}$ (which has more strained or allylic $C_\alpha-N^+$ bonds) than for $\mathbf{1}^{2+}$, +0.22. The charge increase at $C_\alpha H$ of the 21 ring of $\mathbf{10}^{2+}$ is 60% larger, and that at the u22 ring is 22% larger than at $C_\alpha H$ of $\mathbf{1}^{2+}$, rationalizing the significantly more rapid $C_\alpha-N^+$ cleavage reactions observed for compounds containing 21 and unsaturated bicyclic rings.[5]

Dication Optical Spectra

$\mathbf{1}^{2+}$ in acetonitrile shows a broad UV absorption band centered at 230 nm ($\epsilon \sim 5500\ M^{-1}\ cm^{-1}$) and weaker longer wavelength band(s) resulting in nearly constant absorption in the region 295–320 nm ($\epsilon \sim 1700$), tailing to $\epsilon \sim 1000$ at 344 nm (see Figure 1). Similar spectra are exhibited by BF_4^- and PF_6^- salts,[1a] and we attribute these absorptions to the diazenium dication. $\mathbf{1}^{2+}$ shows longer-wavelength absorption than does the radical cation. The longest-wavelength band in hydrazine radical cations is caused by the $\pi \rightarrow \pi^*$ transition,[16] and that of $\mathbf{1}^{\bullet+}$ appears at 265 ± 1 nm for the PF_6^-, BF_4^-, and NO_3^- salts in acetonitrile.[1c] We had expected the $\pi \rightarrow \pi^*$ transition energy for $\mathbf{1}^{2+}$ to be significantly higher than that for $\mathbf{1}^{\bullet+}$ because the $\pi(NN)^*$ orbital is unoccupied for the former and half-filled for the latter. Calculations indicate that this qualitative assumption may be incorrect.

The D_{2h} symmetry of $\mathbf{1}^{2+}$ requires that only *ungerade* symmetry orbitals can have nonvanishing transition moments and hence detectable oscillator strengths, OS, with the *gerade* $\pi^*(NN)$ lumo, which has B_{2g} symmetry. Table 5 shows the orbital energies calculated for $\mathbf{1}^{2+}$ by various methods. The *ab initio* and AM1 calculations agree that the three highest occupied orbitals are heavily $C_\beta H_2$-centered ones of A_u, B_{3g}, and B_{2g} symmetry, and the next set of five occupied orbitals includes four hydrocarbon-centered σ orbitals (three of which are u and one g) and the $\pi(NN)$ orbital, which is of B_{2u} symmetry. This π orbital is highly delocalized over all the heavy atoms, and AM1 gives it only 21% centered at the two nitrogens. The different calculations stir up the relative orbital energies quite thoroughly. It is well-known that transition energies do not correspond to calculated energy gaps between orbitals of different occupancy. Extensive configuration interaction (CI) is involved in optical transitions, and experimental transition energies therefore are very different from the orbital energy gaps calculated between pairs of filled and virtual orbitals. Calculating optical spectra for compounds as large as $\mathbf{1}^{2+}$ from *ab initio* wave functions is very time-consuming, and we have not attempted it. We have carried out AM1-CI calculations, which we hoped would work acceptably for $\mathbf{1}^{2+}$ because AM1 does a rather good job of calculating the geometry. Clark and Chandrasekhar have developed a convenient CI method (which we will call CC-CI) for calculating the wavelengths and oscillator strengths of electronic transitions in organic molecules from AM1 (and other NDDO-based) calculations.[17] They point out that the wide-spread opinion that CI calculations are invalid to consider for NDDO-based semiempirical methods is incorrect, and they argue that use of CI for NDDO-based calculations usefully analyzes state-mixing effects. They also point out that CI calculations play significantly different roles for semiempirical and *ab initio* calculations. CI effects on *ab initio* calculations are dominated by what Sinanoglu calls dynamic correlation effects, arising from the overestimation of electron, electron repulsion in the mean field approximation.[17] Semiempirical calculations are argued to have small dynamic correlation effects for technical reasons and CI calculations based on semiempirical wave functions to emphasize the nondynamic correlations, focusing on state-mixing effects. The CC-CI method employs single and pair-double excitations over a variable-sized active space (PECI is the keyword in their program referring to the number of orbitals centered upon the homo which are mixed in the CI calculation; PECI = 2 includes the highest occupied molecular orbital, homo, and lowest unoccupied orbital, lumo, while PECI = 10 includes [homo−4] to [lumo+4]). They show that for a series of both non-aromatic and aromatic compounds, the CI calculation typically converged at PECI = 8 or 10, and that AM1 CC-CI calculations of the optical spectra for the molecules they considered were rather successful.[17]

Table 5. Comparison of Orbital Energies (eV) Calculated for $\mathbf{1}^{2+}$ (D_{2h} Symmetry)

	RHF/6-31G*	MP2/6-31G*	AM1
[lumo+4}	$-1.19\ B_{1u} = \sigma^*$	$-1.30\ B_{1u} = \sigma^*$	$-5.40\ B_{1g}$
lumo+3]	$-1.26\ A_g$	$-1.36\ A_g$	$-6.22\ B_{3u}$
[lumo+2]	$-1.85\ A_g$	$-1.61\ A_g$	$-8.00\ A_g$
[lumo+1]	$-2.80\ A_g$	$-2.89\ A_g$	$-9.27\ B_{1u} = \sigma^{*\,b}$
lumo	$-7.97\ B_{3g} = \pi^*$	$-8.83\ B_{3g} = \pi^*$	$-10.91\ B_{3g} = \pi^{*\,c}$
homo	$-20.51\ B_{2g}$	$-20.30\ A_u$	$-19.09\ A_u{}^d$
[homo−1]	$-20.55\ A_u$	$-20.65\ B_{2g}$	$-19.20\ B_{3g}{}^d$
[homo−2]	$-20.84\ B_{3g}$	$-20.77\ B_{3g}$	$-19.34\ B_{2g}{}^d$
[homo−3]	$-21.11\ B_{3u}$	$-21.18\ B_{3u}$	$-20.09\ B_{1u}{}^d$
[homo−4]	$-21.26\ A_g$	$-21.23\ B_{2u} = \pi$	$-20.12\ A_g{}^e$
[homo−5]	$-21.93\ B_{1u}$	$-21.31\ A_g$	$-20.16\ B_{3u}{}^e$
[homo−6]	$-21.99\ B_{2u} = \pi$	$-21.84\ A_u$	$-20.29\ A_u{}^e$
[homo−7]	$-22.02\ A_u$	$-21.89\ B_{1u}$	$-21.03\ B_{2u} = \pi^f$

[a] Gaussian calculations select the z axis bisecting the NN bond in the plane of the C_α's, and AM1 perpendicular to this plane (switching B_2 and B_3). We report symmetries here using the Gaussian orientation. [b] An NC_α σ^* combination, centered 92% at N and C_α. [c] π^*, centered 83% at N p_x. [d] homo to [homo−3] are σ combination orbitals centered >80% at the $C_\beta H_2$ groups. [e] [homo−4] to [homo−6] are σ combination orbitals centered >84% at $C_\alpha H$ and $C_\beta H_2$ groups. [f] π, centered 85% at N and C p_x orbitals (0.21 at N, 0.24 at $C_\alpha p_x$, 0.40 at $C_\beta p_x$).

The results of CC-CI calculations on $\mathbf{1}^{2+}$ as a function of active space size are summarized in Table 6. Rather large active space size is required to allow the π orbital to mix with π^*, and there is about a 1 kcal/mol increment in $\Delta\Delta H_f$ when this mixing is allowed. New bands appear when the active space is enlarged to allow mixing of lower-lying occupied orbitals, but the transition energies and oscillator strengths for the other bands are affected little. The experimental spectrum is in acetonitrile, while the CC-CI calculations are for the gas phase. Timothy Clark was kind enough to run a self consistent reaction

---

(16) Nelsen, S. F.; Blackstock, S. C.; Yumibe, N. P.; Frigo, T. B.; Carpenter, J. E.; Weinhold, F. *J. Am. Chem. Soc.* **1985**, *107*, 143.

(17) Clark, T.; Chandrasekhar, J. *Isr. J. Chem.* **1993**, *33*, 435.

Table 6. Summary of CC-CI AM1 Calculations of Optical Transitions for $\mathbf{1}^{2+}$ as a Function of Active Space[a] Size with λ_{max} (OS) in nm Pairs Shown for Each Calculated Transition

active space[a]	$\Delta\Delta H_f$,[b] kcal/mol	homo → lumo(π^*)	[h−3] → π^*	[h−6] → π^*	[h−7](π) → π^*	[h−1] → lumo+1(σ^*)	[h−2] → σ^*
[homo−1]	0.0	353(0.03)				230(0.03)	
[homo−3]	0.1	353(0.03)	276(0.03)			230(0.04)	231(0.26)
[homo−5]	0.2	353(0.04)	276(0.03)			230(0.04)	232(0.22)
[homo−7]	1.3	352(0.06)	273(0.02)	265(0.12)	242(0.20)	229(0.04)	226(0.40)
[homo−9]	1.8	350(0.07)	272(0.02)	264(0.11)	242(0.17)	237(0.04)	228(0.42)
[homo−11]	1.9	350(0.07)	278(0.02)	264(0.12)	244(0.16)	238(0.04)	228(0.41)
[homo−13]	2.1	350(0.07)	272(0.02)	264(0.11)	245(0.17)	238(0.04)	231(0.38)
[homo−15]	2.3	350(0.07)	274(0.02)	265(0.08)	246(0.17)	239(0.04)	232(0.41)
"{CH_3CN}[c]		328(0.07)	260(0.03)	253(0.08)	240(0.17)	231(0.04)	226(0.39)

[a] Calculations are identified by the lowest-lying orbital included in the active space for the CI. The active space for the [homo−1] column is [homo−1] to [lumo+1] (PECI = 4), and for the last column, [homo−15] to [lumo+15] (PECI = 32). [b] $\Delta\Delta H_f$ = (ΔH_f without any CI) − (ΔH_f including CI). [c] SCRF calculation; see text.

field calculation[18] for acetonitrile for the largest active space calculation (see the last line of Table 6), which moves all of the transitions to higher energy. The figure shows the transitions and relative intensities predicted by semiempirical calculations superimposed on the experimental spectrum. We believe that the agreement is surprisingly good.

In an attempt to compare the above semiempirical results with those obtained by an *ab initio* method, CIS/6-31G* calculations have been carried out for the more manageable-sized hydrazine dication, that from tetramethylhydrazine (**TMH**$^{2+}$), which is most stable in D_2 symmetry. The orbital ordering for the RHF geometry optimized structures is the same for the four highest occupied MO's, is scrambled for the next five (the energy differences are rather small), and is the same for the nine lowest valence MO's.[19] The ordering of the virtual MO's is completely different past the lumo, which is B_2 (π^*) for both calculations. CIS/6-31G* predicts bands at 151 nm [OS 0.55], $B_3 \rightarrow B_2$ ([$\pi-\sigma_{CH}$] → π^*), and 121 nm [OS 0.25], A(homo−2) → B_2 (σ^*_{CH} → π^*), while CC-CI/AM1 predicts 265 nm [OS 0.37] and 227 nm [OS 0.27], with the same assignments. The very different virtual orbital ordering does not affect these results because the transitions calculated are both to the lumo. The oscillator strengths and ordering are the same for the *ab initio* and semiempirical calculations, but there is a great discrepancy in the predicted transition energies. Experimentally, the radical cations of both systems have $\pi \rightarrow \pi^*$ transitions in the near-UV, with the bicyclic compound blue shifted: **TMH**$^+$ 303 nm (4.09 eV), $\mathbf{1}^+$ 266 nm (4.66 eV).[16] The semiempirical calculations of $\pi \rightarrow \pi^*$ transitions for the dications give the same order, with a rather small blue shift compared to the radical cations: **TMH**$^{2+}$ 265 nm (4.68 eV, +0.59 eV compared to the monocation), $\mathbf{1}^{2+}$ 246 nm (5.04 eV, +0.38 compared to the monocation). The CIS/6-31G* prediction for **TMH**$^{2+}$ of 151 nm (8.21 eV) is in very poor agreement, and appears likely to us to be significantly too high in energy; the $\pi \rightarrow \pi^*$ absorption of **TMH**$^{2+}$ should be red shifted from that of $\mathbf{1}^{2+}$, and the latter experimentally has near-UV absorption, although it is not known that the $\pi \rightarrow \pi^*$ band occurs in this region. Considerably better agreement of a CIS/6-31G* calculation with the experimental absorption spectrum has been observed for the norbornadiene radical cation,[20] making it appear to us that the CIS/6-31G* calculation performs particularly poorly for **TMH**$^{2+}$, possibly because the RHF/6-31G* structure is poor (it certainly is for $\mathbf{1}^{2+}$, as noted above). (**Note Added in Proof**: A CIS/6-31G* calculation has now been obtained on $\mathbf{1}^{2+}$, which predicts ($\pi \rightarrow \pi^*$)-dominated absorption at 175 nm, far from the experimental result.)

We therefore suggest that it is likely that the long-wavelength absorption region observed for $\mathbf{1}^{2+}$ corresponds to the $\sigma \rightarrow \pi^*$ transition calculated to occur in their region, while the more intense shorter-wavelength band may well include the several types of transitions which are calculated to occur in a relatively narrow energy range. The $\pi \rightarrow \pi^*$ band is calculated to occur in this region, but not to be the principal component of the observed absorption because it has a relatively low oscillator strength. We do not doubt that CIS/6-31G* calculations would give different assignments for the shorter wavelength bands of $\mathbf{1}^{2+}$ because the virtual orbital structure by AM1 and *ab initio* calculations is so different. CIS/6-31G* calculations would seem unlikely to predict $\pi \rightarrow \pi^*$ absorption in the near-UV.

The lower (C_s) symmetry 22/32 dication $\mathbf{3}^{2+}$ shows a broader and weaker short-wavelength band peaking about 222 nm ($\epsilon \sim 3100$) and similar broad longer-wavelength absorption to $\mathbf{1}^{2+}$, also with $\epsilon \sim 1700$ near 395 nm and $\epsilon \sim 1000$ at 348 nm. As might be expected, the lower symmetry results in more complex transitions, because fewer orbitals are symmetry-restricted from mixing, and bands are calculated in similar spectral regions.[21]

Lifetime difficulties have precluded very accurate optical spectral measurements for other tetraalkyldiazenium dications, which were generated in solution by $NOPF_6$ oxidation and studied rapidly. The saturated compounds $\mathbf{5}^{2+}$ (21/22), $\mathbf{11}^{2+}$ (21/23), and $\mathbf{4}^{2+}$ (22/24) all have long-wavelength absorption maxima near about 310 nm, and appear to have somewhat lower ϵ than $\mathbf{3}^{2+}$. The unsaturated compounds $\mathbf{7}^{2+}$ (22/u22) and $\mathbf{12}^{2+}$ (22/u23) both show weak absorption with a maximum about

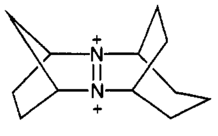

$\mathbf{11}^{2+}$

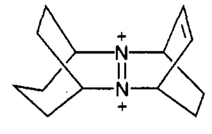

$\mathbf{12}^{2+}$

---

(18) Rauhut, G.; Clark, T.; Steinke, T. *J. Am. Chem. Soc.* **1993**, *115*, 9174.

(19) (a) Gaussian *ab initio* calculations choose the principal axis as bisecting the NN bond perpendicular to the heavy atom plane, while AM1 calculations choose it as the NN bond axis. This switches the symmetry assigned between B_1 and B_3. Because the rule for choosing the principal axis when no other criterion is available is supposed to be to include the most atoms, we use the AM1 orientation for the symmetries quoted below. (b) For D_2 $Me_4N_2^{2+}$ the RHF calculations of valence orbitals from most stabilized to least are as follows: 9 lowest (same order for 6-31G* and AM1): A, B_1, B_2, A, B_3, B_1, A, B_3, B_2; next 5 (scrambled; 6-31G*[AM1]): B_2 [B_3], A [B_2], B_1 [A], B_1 [B_1], B_3 [B_1]; 4 highest (same order for 6-31G* and AM1): B_2, A, B_3, $B_3(\pi-\sigma_{CH})$. Virtual orbitals (6-31G*[AM1]): B_2 [B_2], A [B_1], A [B_3], B_2 [A], B_1 [B_1], B_2 [B_3], B_1 [B_2], B_3 [A], A [B_3], B_1 [B_2].

(20) (a) λ_{max} for the norbornadiene radical cation is 635 nm (1.95 eV),[20b] while a CIS/6-31G* calculation predicts 550 nm (2.25 eV),[20c] 15% too high a transition energy. The transition energy predicted for $Me_4N_2^{2+}$ by CIS/6-31G* is 75% higher than that by CC-CI/AM1. (b) Haselbach, E.; Bally, T.; Lanyiova, Z.; Baertschi, P. *Helv. Chim. Acta* **1979**, 583. (c) Clark, T. Private communication, paper in preparation.

420 nm ($\epsilon \sim 300$ for the more stable compound, $\mathbf{12}^{2+}$), suggesting that the forbidden $\pi(CC),\pi(NN)^*$ transition is that being observed. Although $\mathbf{12}^{2+}$ is calculated by AM1-CC-CI to have a very weak band corresponding principally to a $\pi(CC),\pi(NN)^*$ transition at 459 nm (OS 0.004), the corresponding transition for $\mathbf{7}^{2+}$ is calculated to have OS of 0.000.

Summary

Ab initio calculations show that the charge at nitrogen in $\mathbf{1}^{2+}$ is small, approximately 0.06 to 0.07, so 93–94% of the overall charge of +2 is delocalized onto the alkyl substituents. Double electron removal from $\mathbf{1}^{0}$ results in removal of approximately 1 to 0.9 of an electron from both nitrogens and 0.8 to 0.9 of an electron from the $C_\beta H_2$ groups, rationalizing the remarkably high C_β–H acidity of $\mathbf{1}^{2+}$. AM1 calculations do a surprisingly good job at predicting the geometry of $\mathbf{1}^{2+}$, and AM1 calculations of the optical spectrum which include extensive configuration interaction and an SCRF model for solvent effect do a rather good job of predicting the UV spectrum for this unusual molecule. CIS/6-31G* calculations on $\mathbf{TMH}^{2+}$ predict its $\pi \rightarrow \pi^*$ transition at 151 nm, which is in very poor agreement with the CC-CI calculation of 265 nm.

Experimental Section

Compound preparation has been published separately.[1,5] Acetonitrile was distilled from P_2O_5, deaerated with argon, and passed through activated neutral alumina prior to use. A Hewlett Packard 8452A diode array spectrophotometer was used to record optical spectra. Calculations[22] were carried out on Stardent 3000 and IBM RS-6000 computers.

Acknowledgment. We thank Timothy Clark both for providing VAMP 5.0[22b] as well as assistance with using this package properly and for carrying out the large CIS/6-31G*, CC-CI/AM1, and SCRF calculations,[22d] Peter Petillo for help with implementing Gaussian 92 calculations, and both, as well as Frank Weinhold, for helpful discussions. We thank a referee for valuable comments and the National Science Foundation and the National Institutes of Health for partial financial support of this work under grants CHE-9105485 and GM-29549, respectively, as well as the NSF for funds used in purchasing computers.

JA941853S

---

[21] For an active space including [homo−5] to [lumo+5], the two long-wavelength bands predicted for $\mathbf{1}^{2+}$ (353 nm (0.030) homo → π^* and 276 nm (0.024) 99% [homo−3] → π^*) are replaced by five bands at 341 (0.027), 328 (0.013), 319 (0.038), 316 (0.009), and 302 (0.019), which are significantly more complex, with contributions from two to four ground state orbitals.

[22] (a) *Gaussian 92*: Rev. A., Frisch, M. J.; Trucks, G. W.; Head-Gordon, M.; Gill, P. M. W.; Wong, M. W.; Foresman, J. B.; Johnson, B. G.; Schlegel, H. B.; Robb, M. A.; Replogle, E. S.; Gomperts, R.; Andres, J. L.; Raghavachari, K.; Binkley, J. S.; Gonzalez, C.; Martin, R. L.; Fox, D. J.; Defrees, D. J.; Baker, J.; Stewart, J. J. P.; Pople, J. A.; Gaussian Inc.: Pittsburgh, PA, 1992. (b) *AM1*: Dewar, M. J. S.; Zoebisch, E. G.; Healey, E. F.; Stewart, J. J. P. *J. Am. Chem. Soc.* **1985**, *107*, 3902. (c) Our AM1 and CC-CI[17] calculations employed VAMP 5.0, as supplied modified for use on a Stardent computer by Timothy Clark. Rauhut, G.; Chandrasekhar, J.; Alex, A.; Steinke, T.; Clark, T. *VAMP 5.0*; Oxford Molecular: Oxford, 1994. (d) The PECI > 10 calculations done by Timothy Clark in Erlangen used a newer version of VAMP: Beck, B.; Rauhut, G.; Saver, W.; Chandrasekhar, J.; Clark, T. *VAMP 5.5*; Oxford Molecular: Oxford, 1994.